Behavior of susceptible-infected-susceptible epidemics on heterogeneous networks with saturation

Jaewook Joo
Department of Physics, Rutgers University, Piscataway, New Jersey 08854, USA

Joel L. Lebowitz
Department of Mathematics and Physics, Rutgers University, Piscataway, New Jersey 08854, USA
(Received 3 February 2004; published 2 June 2004)

We investigate saturation effects in susceptible-infected-susceptible models of the spread of epidemics in heterogeneous populations. The structure of interactions in the population is represented by networks with connectivity distribution $P(k)$, including scale-free (SF) networks with power law distributions $P(k) \sim k^{-\gamma}$. Considering cases where the transmission of infection between nodes depends on their connectivity, we introduce a saturation function $C(k)$ which reduces the infection transmission rate λ across an edge going from a node with high connectivity k. A mean-field approximation with the neglect of degree-degree correlation then leads to a finite threshold $\lambda_c > 0$ for SF networks with $2 < \gamma \leqslant 3$. We also find, in this approximation, the fraction of infected individuals among those with degree k for λ close to λ_c. We investigate via computer simulation the contact process on a heterogeneous regular lattice and compare the results with those obtained from mean-field theory with and without neglect of degree-degree correlations.

DOI: 10.1103/PhysRevE.69.066105 PACS number(s): 89.75.−k, 87.23.Ge, 05.70.Ln

I. INTRODUCTION

Many social, biological, and physical systems can be modeled as networks, i.e., connected graphs with at most a single edge between nodes: nodes represent entities and edges represent interaction pathways among the nodes [1,2]. The connectivity pattern in these networks encode information about the structure of the system [3–5]. An important and much studied feature of these networks is their degree distribution $P(k)$, where $P(k)$ is the fraction of nodes of the network that have k connections to other nodes. It was found that many interesting networks such as the internet [6] and the patterns of human sexual contacts [7] are very heterogeneous with approximately scale-free (SF) degree distribution: i.e., $P(k) \sim k^{-\gamma}$ (power law distribution) with $2 < \gamma \leqslant 3$ [6–9]. The study of epidemics in heterogeneous networks is therefore of practical importance for the control of the spread of cyber viruses and biological epidemics.

The mathematical studies of epidemics on the other hand often make the assumption of a homogeneous population [10,11]. This means that any infective individual is an equally likely source for the further transmission of the disease to other members of the population with whom that individual is in contact and vice versa. The simplest epidemiological model of that kind is the susceptible-infected-susceptible (SIS) model [10,11]. In the SIS model, individuals can only exist in two discrete states; healthy (but susceptible) or infected. The disease processes are specified as follows: Infected individuals become susceptible (healthy) at rate δ, independently of their environment. We shall choose time units in which $\delta = 1$. Susceptible individuals become infected at a rate λ multiplied by the number of infected neighbors, i.e., infected nodes to which they are connected by an edge. When the web of interactions between individuals is taken to be a regular lattice the stochastic process describing this system is the Harris' contact process [12].

Epidemic behavior in these homogeneous networks, where each node has z neighbors, $P(k) = \delta_{k,z}$, show a "phase transition" as the rate λ at which an infected individual infects a susceptible neighbor, is changed; i.e., there exists a critical value $\lambda = \lambda_c > 0$ below which the only stationary state is a disease-free state (or absorbing phase) and above which there is an endemic infected state (or active phase). This can be proven rigorously for the stochastic contact process on a regular lattice, an infinite homogeneous network, and is inherited by mean-field models based on this process. The mean-field critical value, λ_c^{MF}, is proportional to z^{-1}, the inverse of the number of "interacting neighbors" [12,13]. This mean field λ_c^{MF} is smaller than that for the contact process. The latter depends not only on the number of neighbors but also on the topology of the lattice (see later) [12,13].

An interesting question then is how to extend these models, which correspond to networks with homogeneous connectivity, to real world situations where the number of contacts varies greatly from one node to another [3–9]. In such heterogeneous networks, each node has a statistically significant probability of having a very large number of connections compared to the average connectivity of the network. The mean-field version of this problem was studied in Refs. [10,14–18] where it was shown that the epidemic threshold decreases with increasing second moment of the connectivity distribution. As a result epidemic processes in infinite SF networks with diverging second moment, $\gamma \leqslant 3$, are believed not to possess any epidemic threshold below which the infection cannot produce an epidemic outbreak or an endemic infected state [14–18].

The absence of an epidemic threshold in SF networks makes them very vulnerable. This remains true even if one takes into account the finite size of real systems which of course always have finite second moments. In general the epidemic threshold for a heterogeneous network is much smaller than for a homogeneous network with the same average number of contacts [19]. The presence of "assortative" or "dissortative" two-point degree correlation in SF networks

with $2<\gamma\leqslant 3$ does not appear to alter the absence of epidemic threshold [20,21].

In these analyses all edges are treated in the same way. There are however many situations where there are differences between the "strength" of different edges. We investigate here cases where the assigned weight of an edge between two nodes depends on the connectivity of these nodes. We consider, in particular, saturation effects due, for example, to the fact that disease transmission requires a certain amount of contact time or "finite time commitment" from both individuals in contact. This has the effect of lowering the effective connectivity for highly connected nodes and thereby decreasing the importance of the "heavy tails" in $P(k)$. Such saturation effects then lead to a finite threshold even when the second moment of $P(k)$ diverges. An example in which saturation effects, due to temporal limitation of interactions, play an important role is Holling's "the principle of time budget" in behavioral ecology [22].

Using mean-field approximations appropriate for heterogeneous network models [15,16] of epidemics we calculate the critical value λ_c for different saturation patterns. We also find in this mean-field approximation, which neglects degree-degree correlations between different nodes, the behavior of the endemic prevalence $\overline{\rho_k}$, i.e., the fraction of infected nodes of degree k, for λ close to λ_c. They all have the same behavior for $\lambda\simeq\lambda_c$, $\overline{\rho_k}\sim A_k(\lambda-\lambda_c)^{\beta}$, with A_k increasing with k; $\beta=1$ when the third moment is finite. This dependence on k is missed by the homogeneous approximation of the contact network.

We then investigate, via numerical simulations, the behavior of the stochastic contact process on a regular lattice consisting of nodes with two different degrees. The results are compared with mean-field approximations with and without neglect of degree-degree correlations.

II. MEAN-FIELD SIS MODEL WITH SATURATION

The mean-field theory for the contact process, obtained by neglecting correlations between different nodes, is described by an equation for the density of infected nodes $\rho(t)$, present at time t, which can be written as [13]

$$\frac{d\rho(t)}{dt}=-\rho(t)+\lambda z\rho(t)[1-\rho(t)], \tag{1}$$

where z is the coordination number. Solving Eq. (1) yields $\rho(t)=(\lambda z-1)\rho(0)e^{(\lambda z-1)t}/[\lambda z-1+\lambda z\rho(0)(e^{(\lambda z-1)t}-1)]$. The steady state solution of Eq. (1), obtained as $t\to\infty$, has an epidemic threshold $\lambda_c^{MF}=1/z$. For $\lambda>\lambda_c^{MF}$, any initial infection spreads and becomes persistent with stationary total prevalence level $\overline{\rho}=(\lambda-\lambda_c^{MF})/\lambda$. Below the threshold $(\lambda<\lambda_c^{MF})$, the initial infection dies out exponentially fast. A similar transition occurs for the stochastic contact process on a regular lattice with edges between nearest neighbors. The critical values λ_c for the lattice $\boldsymbol{Z}^d$ are $\lambda_c\simeq 1.6489$ in one dimension $(d=1,z=2)$, $\lambda_c\simeq 0.4122$ in two dimension $(d=2,z=4)$, etc. $z\lambda_c$ approaches $z\lambda_c^{MF}=1$ as $d\to\infty$ [13].

Consider now a general network with degree distribution $P(k)$. Let $\rho_k(t)$ be the fraction of the nodes with degree k which are infected at time t. We define $\lambda C(k,l)$ as the effective transmission, or infectivity, rate across an edge going from a node with degree k to a node with degree l: $C(k,l)=1$ in the absence of saturation effects.

The mean-field equation of the contact process on this network [15,16], which ignores correlations between the states of the nodes, yields the following set of differential equations for $\rho_k(t)$:

$$\frac{d\rho_k(t)}{dt}=-\rho_k(t)+\lambda Q_k(t)[1-\rho_k(t)]. \tag{2}$$

We can interpret $\lambda Q_k(t)$ as the effective transmission rate of infection to an uninfected node of degree k by all infected nodes with which it is in contact via any of its k edges,

$$Q_k(t)=k\sum_l P(l|k)C(k,l)\rho_l(t). \tag{3}$$

Here $P(l|k)$ is the probability that an edge emerging from a node of degree k has its other end at a node with degree l and $C(k,l)$ is the effective strength of such a bond. We shall now assume further that

$$P(l|k)=\frac{lP(l)}{z} \tag{4}$$

with $z=\Sigma_k kP(k)$, i.e., random attachment (no degree-degree correlation).

To specify $C(k,l)$ in Eq. (3), we make the simplifying assumption that an individual with k contacts spends equal time with each neighbor. The effective strength of an edge is then given by a product of ratios of effective connectivity to total connectivity of each node in contact,

$$C(k,l)=\frac{C(k)C(l)}{kl} \tag{5}$$

with $C(k,l)=1$ corresponding to uniform bond strength.

Equation (2) can now be written in the form

$$\frac{d\rho_k(t)}{dt}=-\rho_k(t)+\lambda[1-\rho_k(t)]C(k)\Theta(\{\rho(t)\}), \tag{6}$$

where

$$\Theta(\{\rho(t)\})=\frac{\sum_k P(k)C(k)\rho_k(t)}{z}. \tag{7}$$

Multiplying Eq. (6) by $C(k)P(k)/z$ and summing over k yields

$$\frac{d\Theta(t)}{dt}=-\Theta(t)+\frac{\lambda\Theta(t)}{z}\sum_k P(k)C^2(k)[1-\rho_k(t)], \tag{8}$$

where $\Theta(t)$ is shorthand for $\Theta(\{\rho(t)\})$. Given $P(k)$ and $C(k)$, Eqs. (6)–(8) form a closed set of nonlinear differential equations for the $\rho_k(t)$ which can be solved, in principle, for any given initial values $\{\rho_j(0)\}$. They reduce to a single equation, Eq. (1), when $P(k)=\delta_{k,z}$ and $\rho_z=\rho$. For a general $P(k)$ the number of variables and equations are infinite.

We are interested primarily in finding stationary solutions $\overline{\rho_k}$, $0 \leqslant \overline{\rho_k} \leqslant 1$, in which not all $\overline{\rho_k}=0$. (There is of course always one solution corresponding to the uninfected state $\rho_k(t)=\rho_k(0)=0$ for all k.) We write the stationary version of Eq. (6) in the form

$$\overline{\rho_k} = \frac{C(k)\lambda\overline{\Theta}}{1 + C(k)\lambda\overline{\Theta}}. \tag{9}$$

Multiplying Eq. (9) by $P(k)C(k)/z$ and summing over k we get

$$\frac{1}{\lambda} = \frac{1}{z}\sum_k P(k)\left[\frac{C^2(k)}{1 + C(k)\lambda\overline{\Theta}}\right] \equiv f(\lambda\overline{\Theta}), \tag{10}$$

where $f(x)$ is a monotone decreasing function of x. Equation (10) will have a (unique) solution $\overline{\Theta}(\lambda)$ different from zero if and only if $\lambda > \lambda_c$, the epidemic threshold,

$$\lambda_c = \frac{1}{f(0)} = \frac{z}{\langle C^2(k)\rangle}. \tag{11}$$

For diverging second moment, $\langle C^2(k)\rangle = \infty$, $\lambda_c = 0$. For a regular lattice with $P(k)=\delta_{k,z}$ and $C(k)=k$, we recover the usual mean-field result, $\lambda_c = 1/z$.

Once we have found $\overline{\Theta}(\lambda) > 0$ from Eq. (10) we then get $\overline{\rho_k}(\lambda) > 0$ directly from Eq. (9) for all k for which $C(k) > 0$. To get the behavior of the $\overline{\rho_k}(\lambda)$ for $\lambda \downarrow \lambda_c$ we expand the right-hand side of Eq. (10) in small $\lambda\overline{\Theta}$. This yields

$$\frac{1}{\lambda} = \frac{1}{\lambda_c} - \frac{\lambda\overline{\Theta}}{z}\sum_k P(k)C^3(k) + O((\lambda\overline{\Theta})^2). \tag{12}$$

Solving for $\overline{\Theta}$ with finite $\langle C^3(k)\rangle$, we get

$$\overline{\Theta}(\lambda) = \frac{z}{\langle C^3(k)\rangle}\left(\frac{1}{\lambda\lambda_c} - \frac{1}{\lambda^2}\right) + \cdots \simeq A(\lambda - \lambda_c) \tag{13}$$

and we obtain from Eq. (9),

$$\overline{\rho_k} \simeq \lambda_c C(k) A(\lambda - \lambda_c), \tag{14}$$

$$\overline{\rho} = \sum_k P(k)\overline{\rho_k} \sim \lambda_c \langle C(k)\rangle A(\lambda - \lambda_c), \tag{15}$$

where $A = z/\lambda_c^3\langle C^3(k)\rangle$.

When $\langle C^3(k)\rangle = \infty$ both $\overline{\Theta}$ and $\overline{\rho}$ are not differentiable as λ approaches λ_c from above. For a SF network with $C(k)=k$, $\langle C^3(k)\rangle$ is finite only for $\gamma > 4$ where $\overline{\rho} \sim (\lambda - \lambda_c)$. However for SF network with connectivity saturation, the range of γ where $\langle C^3(k)\rangle$ is finite can include all cases with $\gamma > 2$ so that z is finite. The case where $\langle C^3(k)\rangle$ is infinite is discussed in the Appendix.

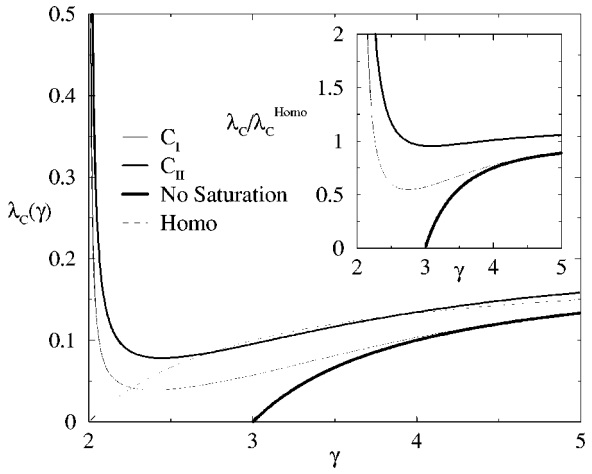

FIG. 1. Epidemic thresholds λ_c as a function of γ. Thin and thick solid lines are drawn for epidemic thresholds from SF networks with saturation type C_I and C_{II}, respectively. Fat solid line represents the epidemic threshold from SF network without saturation. The dashed line is the epidemic threshold for a homogeneous network with coordination number $z=\langle k\rangle$. Inset: Ratios of the epidemic thresholds for the SF network with saturation and without saturation to that of the homogeneous network. $k_{max}=100$, $m=5$, and $p=1$ are used.

III. EPIDEMIC THRESHOLD IN SF NETWORK WITH CONNECTIVITY SATURATION

To see how connectivity saturation modifies the behavior of epidemics, we consider two different types of saturating functions of $C(k)$,

$$C_I(k) = \begin{cases} k & \text{if } k < k_{max} \\ k_{max} & \text{if } k \geqslant k_{max} \end{cases}, \tag{16}$$

$$C_{II}(k) = \frac{k^p k_{max}}{k_{max} + k^p} \quad \text{with} \quad \frac{1}{2} < p \leqslant 1, \tag{17}$$

where k is total connectivity of a node and k_{max} is a parameter.

We replace the sum in Eq. (10) by an integral over k and carry out calculations of λ_c for SF networks with $P(k) = (\gamma - 1)m^{\gamma-1}k^{-\gamma}$ for $k \geqslant m$, $\gamma > 2$. After elementary integration we can obtain the epidemic thresholds λ_c by using Eq. (11) and the second order moment $\langle C^2(k)\rangle$. They are plotted against γ in Fig. 1. This figure presents a phase diagram consisting of two phases: a disease-free state below each epidemic threshold curve and an endemic infection state above each curve. Note that λ_c diverges as $\gamma \to 2$ as can be seen from divergence of z in Eq. (11) when $\langle C^2(k)\rangle$ is finite. This can be understood by noting that as the number of edges increases the effective infection rate for any node decreases. Note also that $\lambda_c = 0$ in the absence of saturation for $2 < \gamma \leqslant 3$ because of the divergence of $\langle C^2(k)\rangle$.

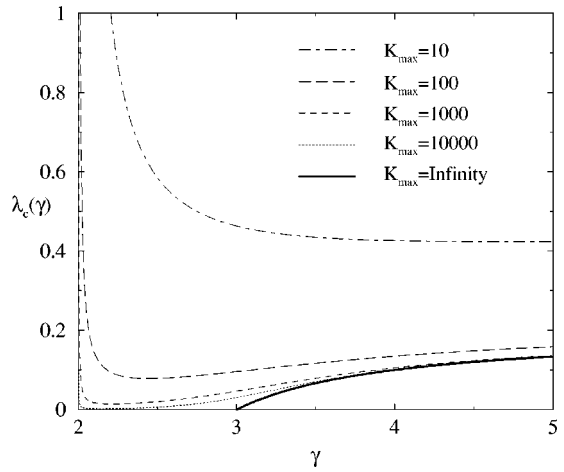

FIG. 2. Dependence of epidemic threshold from SF network with saturation function C_{II} on the cutoff connectivity k_{max}. From top to bottom $k_{max}=10, 10^2, 10^3, 10^4$, and ∞. Here $p=1$ for $C_{II}(k)$.

In the inset of Fig. 1 we compare the epidemic thresholds λ_c of SF networks with saturation with λ_c^{homo}, obtained from a homogeneous network with coordination number $z=\langle k\rangle$.

The dependence of the epidemic threshold on k_{max} is plotted in Fig. 2. When k_{max} is finite, the epidemic threshold $\lambda_c(\gamma)$ is nonzero for $\gamma>2$ and as k_{max} increases $\lambda_c(\gamma)$ decreases. When $k_{max}=\infty$, the epidemic threshold of SF network without saturation is recovered.

The stationary total prevalence $\overline{\rho}$ for the SF network with and without saturation is plotted in Fig. 3. The stationary total prevalence $\overline{\rho}(\lambda)$ with saturation is smaller than that without saturation for all $\lambda>0$. This is because saturation reduces the effective transmission rate of infection to an uninfected node across an edge going from an infected node with high connectivity [see Eqs. (3) and (5)].

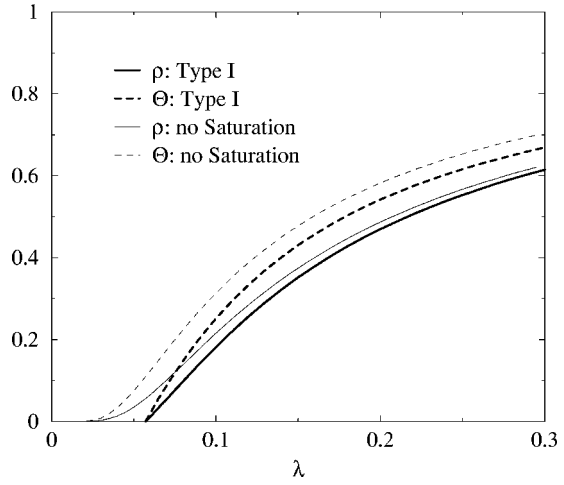

FIG. 3. The steady state $\overline{\rho}(\lambda)$ and $\overline{\Theta}(\lambda)$ of the SIS epidemics on the SF network for $\gamma=3$ as a function of infectivity λ. Thick solid (thick dashed) lines indicate the steady state $\overline{\rho}^{C_I}$ ($\overline{\Theta}^{C_I}$) with type I saturation. Thin lines are for those without saturation. The critical point in this particular case is given: $\lambda_c^{C_I}=0.0573$ for type I saturation and $\lambda_c=0$ for no saturation. Here $k_{max}=100$ and $m=5$ are used.

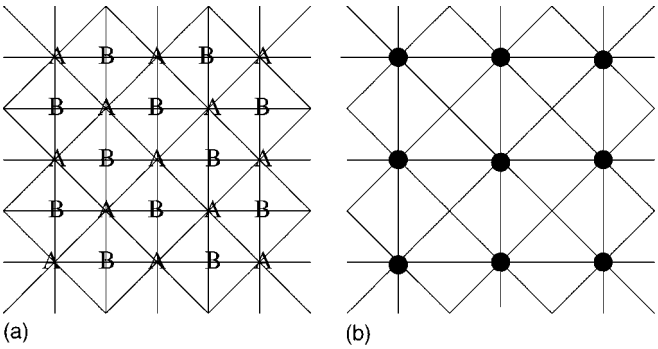

FIG. 4. The topology of lattices. (a) The face-centered square (FCS) lattice. Nodes with type A have eight degrees while nodes with type B have four degrees. (b) A homogeneous network with $z=8$.

IV. THE CONTACT PROCESS AND MEAN-FIELD APPROXIMATION IN A HETEROGENEOUS REGULAR LATTICE

To investigate the effect of heterogeneity and degree-degree correlations we investigated the SIS model on the "face-centered" square (FCS) lattice with two types of nodes. Type *A* nodes, which connect to both nearest and next nearest neighbor sites, have connectivity $k_A=8$ and type *B*, which connect only to nearest neighbor sites, have $k_B=4$. For this system $P(8|4)=1$ and $P(4|8)=P(8|8)=1/2$, and $P(k_\gamma|k_\alpha)=0$ otherwise, see Fig. 4.

We carried out computer simulations on this model with no saturation. The critical point λ_c and critical exponents, δ, $\nu_\parallel$, and $\nu_\perp$, were obtained by using the dynamical Monte Carlo method [23]. As expected there is a critical point $\lambda_c=0.23(6)$. This value of λ_c is closer to $\lambda_c=0.18(1)$ for the homogeneous regular lattice with $z=8$ than to $\lambda_c=0.412$ [13] for the square lattice with $z=4$. The homogeneous regular lattice with $z=8$ is the square lattice with both nearest neighbor (NN) and next NN bonds (see Fig. 4). The critical exponents appear to be the same as for the square lattice as expected from universality considerations. The phase diagram is plotted in Fig. 5.

We also computed $\overline{\rho_A}$ and $\overline{\rho_B}$ for $\lambda>\lambda_c$. The results are plotted in Fig. 6. We can see that nodes with higher connectivity are more infected than those with less connectivity at λ close to λ_c.

The mean-field equations of the SIS on this lattice with the exact $P(k_\gamma|k_\alpha)$ are

$$\frac{d\rho_A}{dt}=-\rho_A+4\lambda(1-\rho_A)(\rho_A+\rho_B), \tag{18}$$

$$\frac{d\rho_B}{dt}=-\rho_B+4\lambda\rho_A(1-\rho_B). \tag{19}$$

The steady state solutions are given,

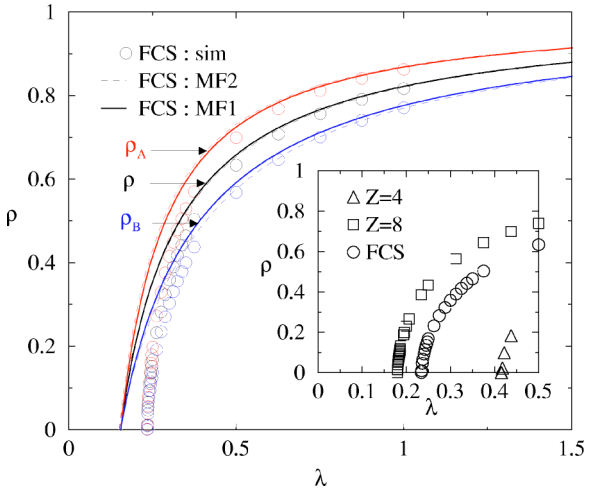

FIG. 5. The steady state prevalence $\overline{\rho}$ of SIS in the FCS lattice without saturation as a function of infectivity rate λ. $\overline{\rho_A}(\overline{\rho_B})$ represents the fraction of infected nodes of type A and type B, respectively, and $\overline{\rho}=(\overline{\rho_A}+\overline{\rho_B})/2$. Simulation (sim) data are shown with circles while mean-field results, where MF1 with exact $P(k_\gamma|k_\alpha)$ and MF2 with the approximate one using Eq. (4), are given with solid and dashed lines, respectively. Inset: Simulation results of the contact process in the FCS lattice (circles), in the square lattice (triangles) with $z=4$ and in the square lattice with both nearest and next nearest neighbor interactions (squares) with $z=8$. All simulations were performed on lattices of size $L^2=100^2$ with random initial distribution of infected nodes.

$$\overline{\rho_A}=\frac{\overline{\rho_B}}{4\lambda(1-\overline{\rho_B})},\quad \overline{\rho_B}=1-\frac{1}{2\lambda+4\lambda^2}, \tag{20}$$

with $\lambda_c=(-1+\sqrt{5})/8$. We call this "MF1."

The mean-field equations with "no degree-degree correlation" approximation, "MF2," can be obtained in a similar manner to that given in Eqs. (6) and (7). This corresponds to putting $P(4|4)=P(4|8)=1/3$ and $P(8|4)=P(8|8)=2/3$.

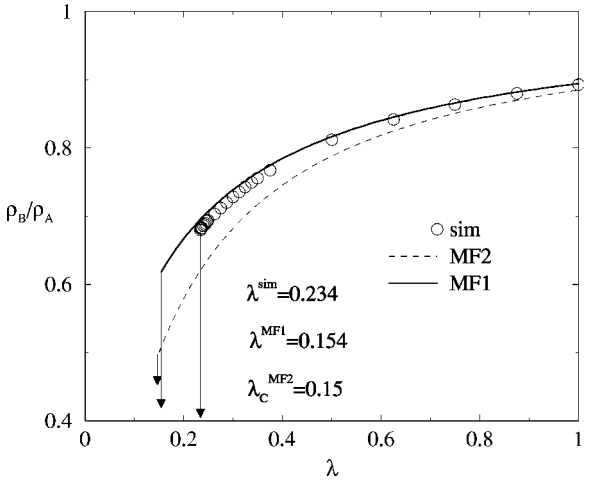

FIG. 6. Ratio of $\overline{\rho_B}$ to $\overline{\rho_A}$ in the FCS lattice as a function of infectivity rate λ. The notation and symbols are the same as in Fig. 4. The arrows point to the critical λ_c corresponding to each scheme.

TABLE I. The critical point λ_c, the ratios $\psi_{A(B)}$ and ϕ, $\psi_{A(B)}=\lim_{\lambda\to\lambda_c}[\overline{\rho}_{A(B)}(\lambda)/(\lambda-\lambda_c)]$ and $\phi=\lim_{\lambda\to\lambda_c}(\overline{\rho_B}/\overline{\rho_A})$, of the SIS epidemics on the face-centered square lattice. "Sim" refers to simulation data without saturation [i.e., $C(k)=k$] while MF1 and MF2 refer to mean-field analysis with exact $P(k_\gamma|k_\alpha)$ and the approximate one using Eq. (4), respectively.

	λ_c	ψ_A	ψ_B	ϕ
Sim	0.23(6)	∞	∞	0.7
MF1	0.15	7.24	4.5	0.62
MF2	0.15	7.4	3.7	0.5

The results from simulation and the two mean-field approximations are compared in Figs. 5 and 6 and in Table I. Close to the critical point, we can approximate the ratio, $\overline{\rho_B}/\overline{\rho_A}$, by neglecting nonlinear term in Eq. (19): $\overline{\rho_B}/\overline{\rho_A}\sim 4\lambda_c P(8|4)/[1-4\lambda_c P(4|4)]$. In this heterogeneous lattice with only two types of nodes, MF2 with no degree-degree correlation gives the same λ_c but not as good values for $\overline{\rho_A}$ and $\overline{\rho_B}$ as MF1 with the exact degree-degree correlation.

V. CONCLUDING REMARKS

In this paper we considered the SIS epidemic model on heterogeneous networks with saturation. This made the epidemic thresholds finite for SF networks with $2<\gamma\leqslant 3$. We also investigated via computer simulation the stochastic contact process on a heterogeneous regular lattice and compared the results with those obtained from mean-field theory with and without neglect of degree-degree correlations. Our considerations extend naturally to other types of heterogeneous networks in which the effective strength of an edge depends on the degrees of the nodes which it connects. Thus in considering the spread of computer viruses on the internet, effects similar to saturation might arise from nodes with high connectivity having higher "firewalls" around them.

ACKNOWLEDGMENTS

J.J. thanks DIMACS for support and acknowledges the support of Grants Nos. NSF DBI 99-82983 and NSF EIA 02-05116. J.J.L. was supported by Grants Nos. NSF DMR-01-279-26 and AFOSR AF 49620-01-1-0154.

APPENDIX: CRITICAL BEHAVIOR OF $\overline{\rho}$ WHEN $\langle C^3(k)\rangle=\infty$

The critical behavior of the steady state $\overline{\Theta}$ and $\overline{\rho}$ in the presence of saturation can be evaluated by using the third order moment $\langle C^3(k)\rangle$. When $k_{max}<\infty$, both $\overline{\Theta}$ and $\overline{\rho}$ can be expanded in a power series close to the critical point because of z, $\langle C_I^3(k)\rangle$ and $\langle C_{II}^3(k)\rangle$ being all finite for $\gamma>2$.

When $k_{max}\to\infty$, $\langle C^3(k)\rangle$ may diverge and as a result the expression of Eqs. (13)–(15) are not valid any more. Let us introduce the limiting case of $C_{II}(k)$ when $k_{max}=\infty$,

$$C_{III}(k) = k^p \quad \text{for } \tfrac{1}{2} < p \leqslant 1. \tag{A1}$$

Then, $\langle C_{III}^n(k)\rangle = (\gamma-1)m^{np}/\gamma - np - 1$ for $\gamma > np+1$ while $\langle C_{III}^n(k)\rangle = \infty$ for $2 < \gamma \leqslant np+1$. When $\gamma > 3p+1$, i.e., $\langle C_{III}^3(k)\rangle < \infty$, $\overline{\Theta}$ and $\overline{\rho}$ at λ close to λ_c are equivalent to those in Eqs. (13)–(15).

However when $2 < \gamma \leqslant 3p+1$, i.e., $\langle C_{III}^3(k)\rangle = \infty$, $\overline{\rho}$ and $\overline{\Theta}$ are treated in different ways and their behaviors close to the critical point are presented as follows: For $C_{III}(k)$ the steady state $\overline{\Theta}^{C_{III}}$ and $\overline{\rho}^{C_{III}}$ can be given,

$$\overline{\Theta}^{C_{III}} = \frac{(\gamma-1)m^p}{z(\gamma-p-1)}\,{}_2F_1\left[1, \eta-1, \eta, -\frac{1}{\lambda\overline{\Theta}m^p}\right], \tag{A2}$$

$$\overline{\rho}^{C_{III}} = {}_2F_1\left[1, \eta, \eta+1, -\frac{1}{\lambda\overline{\Theta}m^p}\right] \tag{A3}$$

for noninteger values of $\eta \equiv (\gamma-1)/p$ and for $\gamma > 2$. After Taylor expansion in the limit of small $\overline{\Theta}$ we obtain (i) $\overline{\rho}^{C_{III}} \simeq \lambda^{(\eta-1)/(2-\eta)}$ for $2 < \gamma \leqslant 2p+1$, (ii) $\overline{\rho}^{C_{III}} \simeq \lambda^{1/(\eta-2)}$ for $2p+1 < \gamma \leqslant 3p+1$.

[1] S. H. Strogatz, Nature (London) **410**, 268 (2001).
[2] D. J. Watts and S. H. Strogatz, Nature (London) **393**, 440 (1998).
[3] R. Albert and A.-L. Barabasi, Rev. Mod. Phys. **85**, 5234 (2000).
[4] S. N. Dorogovtsev and J. F. F. Mendes, Adv. Phys. **51**, 1079 (2002).
[5] M. E. J. Newman, SIAM Rev. **45**, 167 (2003).
[6] M. Faloutsos, P. Faloutsos, and C. Faloutsos, ACM SIGCOMM '99, Comput. Commun. Rev. **29**, 251 (1999).
[7] F. Liljeros, C. R. Edling, L. A. N. Amaral, H. E. Stanley, and Y. Aberg, Nature (London) **411**, 907 (2001).
[8] A.-L. Barabasi and R. Albert, Science **286**, 509 (1999).
[9] R. Albert, H. Jeong, and A.-L. Barabasi, Nature (London) **401**, 130 (1999).
[10] R. M. Anderson and R. M. May, *Infectious Diseases in Humans* (Oxford University Press, Oxford, 1992).
[11] O. Diekmann and J. A. P. Heesterbeek, *Mathematical Epidemiology of Infectious Diseases: Model Building, Analysis and Interpretation* (Wiley, New York, 2000).
[12] T. M. Liggett, *Interacting Particle Systems* (Springer-Verlag, New York, 1959).
[13] J. Marro and R. Dickman, *Nonequilibrium Phase Transitions in Lattice Models* (Cambridge University Press, Cambridge, 1999).
[14] R. M. May and A. L. Lloyd, Phys. Rev. E **64**, 066112 (2001).
[15] R. Pastor-Satorras and A. Vespignani, Phys. Rev. Lett. **86**, 3200 (2001).
[16] R. Pastor-Satorras and A. Vespignani, Phys. Rev. E **63**, 066117 (2001).
[17] M. E. J. Newman, Phys. Rev. E **66**, 016128 (2002).
[18] D. Volchenkov, L. Volchenkova, and P. Blanchard, Phys. Rev. E **66**, 046137 (2002).
[19] R. Pastor-Satorras and A. Vespignani, Phys. Rev. E **65**, 035108 (2002).
[20] M. Boguna, R. Pastor-Satorras, and A. Vespignani, Phys. Rev. Lett. **90**, 028701 (2003).
[21] Y. Moreno, J. B. Gomez, and A. F. Pacheco, Phys. Rev. E **68**, 035103(R) (2003).
[22] C. S. Holling, Canadian Entomologist **91**, 293 (1959).
[23] P. Grassberger and A. de la Torre, Ann. Phys. (N.Y.) **122**, 373 (1979).